

Theory of spoof plasmons in real metals

Anastasia Rusina · Maxim Durach · Mark I. Stockman

Received: 1 February 2010 / Accepted: 1 June 2010
© Springer-Verlag 2010

Abstract In this Letter we develop a theory of spoof plasmons propagating on real metals perforated with planar periodic grooves. Deviation from the spoof plasmons on perfect conductor due to finite skin depth has been analytically described. This allowed us to investigate important propagation characteristics of spoof plasmons such as quality factor and propagation length as the function of the geometrical parameters of the structure. We have also considered THz field confinement by adiabatic increase of the depth of the grooves. It is shown that the finite skin depth limits the propagation length of spoof plasmons as well as a possibility to localize THz field. Geometrical parameters of the structure are found which provide optimal guiding and localization of THz energy.

1 Introduction

Spoof plasmons are bound electromagnetic waves at frequencies outside the plasmonic range mimicking (“spoofing”) surface plasmon polaritons (SPPs), which propagate on the periodically corrugated metal surfaces. The spoof plasmons have first been proposed in Ref. [1] in order to explain extraordinary optical transmission (EOT) through the perforated films [2]. The first experimental demonstration of the spoof plasmons was done using periodically arranged hollow brass tubes [3]. Generally at terahertz (THz) frequencies, there are no SPPs propagating at the metal/dielectric interface due to large free electron density, which places the

surface plasma frequency in the visible or ultraviolet parts of the spectrum. One of the advantages of using fields propagating along corrugated surfaces is their strong coupling to interface at THz frequencies and a possibility to control their dispersion through geometrical parameters of the structure. This has already created a new vibrant field of research [4–11].

To date, theoretical consideration of such an interesting phenomenon as spoof plasmons is mostly based on the perfect metal description [4–8]. Although there have been papers considering spoof plasmon losses, mainly due to diffraction [9, 10], the question of how losses affect propagation and localization of spoof plasmons is still open. The qualitative picture showing the dependence of spoof plasmon propagation on metal skin depth, which in addition to diffraction is the main channel of loss, is needed. It has been recently shown that deviation of real metals from the perfect conductor is important for propagation and localization properties of THz fields [12].

In this Letter, we consider the influence of the metal loss (finite skin depth) on spoof plasmon behavior. We have obtained a simple analytical dispersion relation of the spoof plasmons on the corrugated surface of a real metal. We have shown that their propagation length as well as spatial limit on THz energy concentration by means of spoof plasmons are determined by the metal skin depth.

2 Effective medium approximation

Consider a surface of the metal with dielectric permittivity ε_m perforated with a one-dimensional periodic array of grooves of width a and depth h . The period of the array is d . The material inside the grooves has dielectric function ε_g . The corrugated surface is in contact with a medium with

A. Rusina · M. Durach · M.I. Stockman (✉)
Department of Physics and Astronomy, Georgia State University,
Atlanta, GA 30303, USA
e-mail: mstockman@gsu.edu
url: <http://www.phy-astr.gsu.edu/stockman>

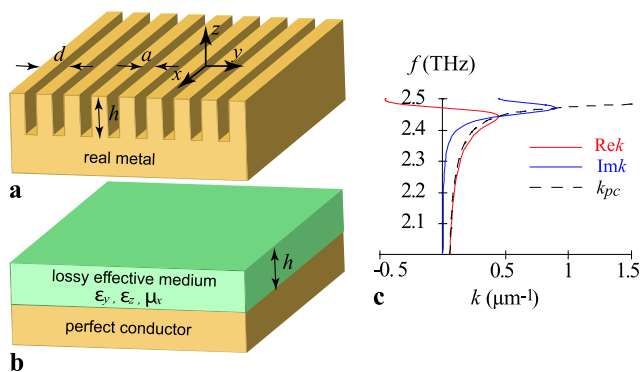


Fig. 1 (a) An array of grooves of width a and depth h cut in real metal with the period of the system d . The metal is placed in dielectric with permittivity ε_d . (b) The structure with grooves in the effective medium approximation. Parameters of the effective medium are given by (1) and (3). (c) The dispersion relation of the spoof plasmons (frequency f versus wave vector k) supported by a 1D array of grooves with geometrical parameters $a/d = 0.3$, $a = 3 \mu\text{m}$, $h = 30 \mu\text{m}$. The real part, $\text{Re}k$, is denoted by the red line and $\text{Im}k$ by the blue line, while the black dashed line is the dispersion relation for a perfect conductor. The dielectric functions ε_d and ε_g are chosen to be one

permittivity ε_d . This structure is shown in Fig. 1(a). Such interface can be modeled as a three-layer structure, consisting of a homogeneous anisotropic layer of thickness h , describing corrugations, placed between the metal and the dielectric, displayed in Fig. 1(b). The approximation of the central layer as an anisotropic effective medium is possible as long as the period d is much smaller than the wavelength of the electromagnetic field.

In order to find the dielectric parameters of the effective medium, consider a periodic assembly of parallel metal plates. The effective dielectric constants of such assembly are [13]

$$\varepsilon_x = \varepsilon_z = \frac{(d-a)\varepsilon_m + a\varepsilon_g}{d}, \quad \varepsilon_y = \frac{d}{(d-a)/\varepsilon_m + a/\varepsilon_g}. \quad (1)$$

The field of spoof plasmons is composed of parallel plate waveguide modes, propagating along the grooves, whose amplitudes are correlated through spoof plasmon phase. Let k be the spoof plasmon wave vector and k_g is the wave vector of the wave propagating into the grooves [12]

$$k_g = k_0 \sqrt{\varepsilon_g} \left(1 + \frac{l_s(i+1)}{a} \right)^{1/2}, \quad (2)$$

where $k_0 = 2\pi f/c$ is the vacuum wave vector, f is the frequency, and $l_s = (k_0 \text{Re} \sqrt{-\varepsilon_m})^{-1}$ is the skin depth of the metal. The magnetic permeability of the effective medium, which allows one to fulfill the effective Maxwell equations,

is the following

$$\mu_x = \frac{1}{k_0^2} \left(\frac{k^2}{\varepsilon_z} + \frac{k_g^2}{\varepsilon_y} \right), \quad (3)$$

where ε_y and ε_z are given by (1). Thus the array of planar grooves cut in non-perfect conductor can be replaced by an anisotropic layer of thickness h with parameters given by (1) and (3).

3 Propagation of terahertz spoof plasmons in real metals

Using the effective medium approximation derived in the previous section, we can describe the transverse magnetic spoof plasmon mode, propagating in the structure. The only non-zero components of the magnetic and electric fields are H_x , E_y , E_z :

$$H_x = A e^{iky} \begin{cases} e^{-\kappa z} & \text{for } z > 0 \\ \frac{\cos(k_g(z+h))}{\cos(k_g h)} & \text{for } -h < z < 0 \end{cases}, \quad (4)$$

$$E_y = -\frac{\partial_z H_x}{ik_0 \varepsilon_y} = -\frac{A i e^{iky}}{k_0} \begin{cases} \frac{\kappa}{\varepsilon_d} e^{-\kappa z} & \text{for } z > 0 \\ \frac{k_g}{\varepsilon_y} \frac{\sin(k_g(z+h))}{\cos(k_g h)} & \text{for } -h < z < 0 \end{cases}, \quad (5)$$

$$E_z = \frac{\partial_y H_x}{ik_0 \varepsilon_z} = \frac{A k e^{iky}}{k_0} \begin{cases} \frac{1}{\varepsilon_d} e^{-\kappa z} & \text{for } z > 0 \\ \frac{\cos(k_g(z+h))}{\varepsilon_z \cos(k_g h)} & \text{for } -h < z < 0 \end{cases}. \quad (6)$$

Here k is the spoof plasmon wave vector, k_g is defined by (2), $\kappa = \sqrt{k^2 - \varepsilon_d k_0^2}$, and A is the amplitude. Note that the region $-h < z < 0$ is occupied by the effective medium; thus, ε_y and ε_z are given by (1). The area $z < -h$ is chosen to be a perfect conductor, so the fields there are zero. This is a good approximation since $a \ll h$, and losses at the bottom of the grooves are negligible.

Matching the fields at the boundary $z = 0$, we obtain the spoof plasmon wave vector as

$$k = \left(\varepsilon_d k_0^2 + \left(\frac{a \varepsilon_d}{d \varepsilon_g} \right)^2 k_g^2 \tan^2(k_g h) \right)^{1/2}. \quad (7)$$

This is the dispersion relation for the spoof plasmons supported by the corrugated surface of a real metal. Equation (7) takes into account the finite conductivity of the metal via k_g (2) that depends on the skin depth l_s . This skin depth is in the range 30–120 nm for the THz part of the spectrum [14].

To illustrate the dependence of the spoof plasmon properties on the metal skin depth, we plot the real and imaginary parts of the wave vector k as the function of frequency f in

Fig. 1(c). The dashed black line in Fig. 1(c) corresponds to the dispersion of spoof plasmons on the perfect conductor. It can be seen that at resonant frequency, which for given parameters is $f \approx 2.5$ THz, the wave vector k_{pc} is infinitely large. However, if losses are taken into account, $\text{Re} k$ (red curve) experiences the backbending similarly to SPPs and has a finite maximum value. Also there is a peak of $\text{Im} k$ (blue curve) near the resonance. The analytical approximation for $\text{Im} k$ can be obtained from analysis of (7)

$$\text{Im} k \simeq \frac{k_0 \varepsilon_d^{3/2}}{2 \varepsilon_g} \zeta(\varepsilon_g^{1/2} k_0 h) \left(\frac{a}{d}\right)^2 \frac{l_s}{a}, \quad (8)$$

where $\zeta(x)$ is a function defined as $\zeta(x) = \tan(x) \times (x \sec^2(x) + \tan(x))$. This expression is an excellent approximation at all frequencies, except for the region of backbending. As one can see from (8), the spoof plasmon propagation length $l_p = 1/(2 \text{Im} k)$ is inversely proportional to the skin depth of the metal and becomes infinite for the perfect conductor. The propagation length is proportional to d^2 in agreement with numerical computation of Ref. [10].

The spoof plasmon figure of merit $Q = \text{Re} k / \text{Im} k$ is depicted in Fig. 2(a) as a function of the geometrical parameters of the system, a and h at $f = 1$ THz. Physically Q shows how many oscillations a spoof plasmon undergoes before it decays. The black curve in this figure shows when $Q = 4\pi$, which corresponds to energy decay length equal to wavelength. The area to the left of this curve is suitable for propagation of THz field with spoof plasmons.

Besides the figure of merit, Q , the other important propagation characteristics of spoof plasmons are the energy attenuation length (propagation length) $l_p = 1/(2 \text{Im} k)$ and the energy confinement in the dielectric $\xi = 1/(2 \text{Re} \kappa)$. In Fig. 2(b), these two parameters are shown as a function of the depth of the grooves, h . Note that the better the confinement is, the lower is the propagation length.

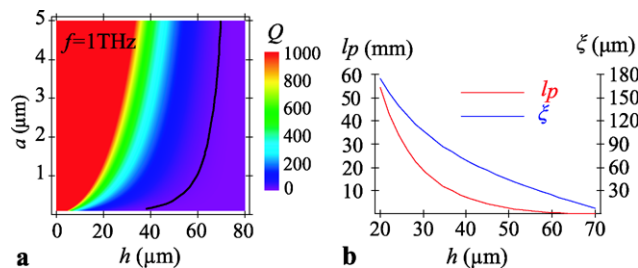


Fig. 2 (a) Spoof plasmon figure of merit Q as a function of a and h for $f = 1$ THz ($a/d = 0.3$). Black curve corresponds to $Q = 4\pi$. (b) The propagation length l_p (red curve) and confinement length ξ (blue curve) of spoof plasmons as functions of the depth of the grooves h at $f = 1$ THz for the parameters $a/d = 0.3$, $a = 3 \mu\text{m}$. Note the different scales on the right and left axes

4 Adiabatic concentration on spoof plasmon structure

The spoof plasmons were proposed as a promising tool for the concentration of THz radiation [7]. However, this assumption was based on the perfect conductor description, which did not take losses into account. Here we consider the possibility of focusing using the non-perfect metal with periodically drilled grooves and show that the concentration is limited to tens of micrometers.

In order to achieve a good focusing and high intensity, the wave vector of the spoof plasmons k given by (7) should be large. It can be seen from (7) that k reaches maximum when the argument under the tangent $k_g h \rightarrow \pi/2$, i.e., the grooves play the role of quarter-wavelength antennas. Because $k_g \approx k_0$, such a resonance occurs when $h \approx \lambda_0/4$. In order to concentrate spoof plasmons one should adiabatically increase the depth of the grooves until the wave vector k reaches maximum. With the intention of achieving the adiabatic concentration using spoof plasmons, one should keep the parameter of the adiabaticity $\delta = |d(\text{Re} k^{-1})/dy|$ small compared to the unity. In the specific computations, we keep $\delta = 0.1$, which allows us to determine the dependence $h(y)$, i.e., the appropriate grading of the groove depth (or, thickness of the effective medium).

Following the well-developed method of the adiabatic concentration [15–17], the phase of the spoof plasmon mode (eikonal) is determined by the following integral $\Phi(y) = \int k(y) dy$, where $k(y)$ is defined by (7). The amplitude of the fields $A(y)$ can be found using the conservation of energy flux. The fields given by (4)–(6) with the phase determined by the eikonal exponent $e^{i\Phi(y)}$ and the amplitude $A(y)$ are plotted in plane yz in Figs. 3(a)–(c). The electric field energy density (see, e.g., Ref. [18])

$$U = \frac{1}{16\pi} \left\{ \text{Re} \left(\frac{d[f \varepsilon_z(f)]}{df} \right) |E_z|^2 + \text{Re} \left(\frac{d[f \varepsilon_y(f)]}{df} \right) |E_y|^2 \right\} \quad (9)$$

is plotted in Fig. 3(d) in relative units. As one can see, when the depth of the grooves h is adiabatically increased (shown by the dashed black line), the density of the spoof plasmons field increases by the factor of 100, while the wavelength decreases from $300 \mu\text{m}$ to $40 \mu\text{m}$, while the THz energy is concentrated.

We have also estimated the minimum size of the hot spot that can be achieved by concentration of the spoof plasmons on real metals. In the case of the perfect conductor, the size of the hot spot is not limited by the losses and can theoretically be arbitrarily small. One can make both the period d and the width of the grooves a infinitesimally small to avoid diffraction. However, if losses are introduced and the skin depth l_s is finite, there is a limitation on the size of the hot

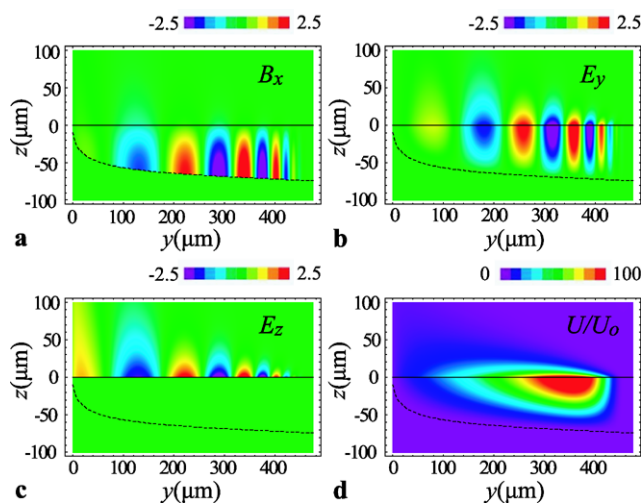


Fig. 3 Terahertz spoof energy concentration due to adiabatic increase of the thickness of the effective medium. **(a)** Instantaneous distribution of transverse magnetic field B_x as the function of the coordinate y along the propagation direction. **(b)** The same as panel **(a)** but for the longitudinal electric field E_y . **(c)** The same as panel **(a)** but for the transverse electric field E_z . The units of the fields are arbitrary but consistent between panels. **(d)** The electric fields density of spoof plasmons U , relative to density U_0 , at the point $(0,0)$ in yz plane, as the function of y . The dashed black line represents the shape of the effective medium, i.e. $h(y)$

spot. In order to have a high wave vector k , one needs to use a strong coupling with the resonance of the grooves. To have a sharp resonance and small spoof plasmon wavelengths, the resonance figure of merit l_s/a should be small. Since for the given frequency the skin depth l_s is fixed, one has to increase the size of the system. On the other hand, the increase of d leads to strong diffraction when d becomes comparable with the wavelength of spoof plasmons. This analysis leads to the minimum achievable hot spot size on the order of 30–40 μm .

5 Conclusion

In this Letter, we have developed a theory, which describes the spoof plasmons propagating on the real metal with the finite skin depth. The derived dispersion relation allowed us to investigate analytically propagation characteristics of the spoof plasmons such as the propagation length, energy confinement size, and figure of merit as functions of the geometrical parameters of the structure. Despite the finite energy dissipation, our selection of the optimum parameters of the structure provides for good guiding and confinement of THz field with spoof plasmons. We have also considered the possibility of adiabatic concentration of THz energy by spoof plasmons. We have shown that the concentration of the spoof plasmons to a spot with the size of 30–40 μm is possible, while their intensity increases by more than two orders of magnitude.

Acknowledgements This work was supported by grants from the Chemical Sciences, Biosciences and Geosciences Division of the Office of Basic Energy Sciences, Office of Science, U.S. Department of Energy, a grant CHE-0507147 from NSF, and a grant from the US-Israel BSF.

References

1. J.B. Pendry, L. Martin-Moreno, F.J. Garcia-Vidal, Mimicking surface plasmons with structured surfaces. *Science* **305**(5685), 847–848 (2004)
2. T.W. Ebbesen, H.J. Lezec, H.F. Ghaemi, T. Thio, P.A. Wolff, Extraordinary optical transmission through sub-wavelength hole arrays. *Nature* **391**, 667–669 (1998)
3. A.P. Hibbins, B.R. Evans, J.R. Sambles, Experimental verification of designer surface plasmons. *Science* **308**(5722), 670–672 (2005)
4. F.J. Garcia-Vidal, L. Martin-Moreno, J.B. Pendry, Surfaces with holes in them: new plasmonic metamaterials. *J. Opt. A, Pure Appl. Opt.* **7**(2), S97–S101 (2005)
5. F.J.G. de Abajo, J.J. Sáenz, Electromagnetic surface modes in structured perfect-conductor surfaces. *Phys. Rev. Lett.* **95**(23), 233901 (2005)
6. Z. Ruan, M. Qiu, Slow electromagnetic wave guided in subwavelength region along one-dimensional periodically structured metal surface. *Appl. Phys. Lett.* **90**(20), 201906 (2007)
7. S.A. Maier, S.R. Andrews, L. Martin-Moreno, F.J. Garcia-Vidal, Terahertz surface plasmon-polariton propagation and focusing on periodically corrugated metal wires. *Phys. Rev. Lett.* **97**, 176805-1-4 (2006)
8. Y. Chen, Z. Song, Y. Li, M. Hu, Q. Xing, Z. Zhang, L. Chai, C. Wang, Effective surface plasmon polaritons on the metal wire with arrays of subwavelength grooves. *Opt. Express* **14**(26), 13021–13029 (2006)
9. L. Shen, X. Chen, Y. Zhongand, K. Agarwal, Effect of absorption on terahertz surface plasmon polaritons propagating along periodically corrugated metal wires. *Phys. Rev. B* **77**, 075408 (2008)
10. L. Shen, X. Chen, T. Yang, Terahertz surface plasmon polaritons on periodically corrugated metal surfaces. *Opt. Express* **16**(5), 3326–3333 (2008)
11. D. Martin-Cano, M.L. Nesterov, A.I. Fernandez-Dominguez, F.J. Garcia-Vidal, L. Martin-Moreno, E. Moreno, Domino plasmons for subwavelengthterahertz circuitry. *Opt. Express* **18**(2), 754–764 (2010)
12. A. Rusina, M. Durach, K.A. Nelson, M.I. Stockman, Nanoconcentration of terahertz radiation in plasmonic waveguides. *Opt. Express* **16**(23), 18576–18589 (2008)
13. M. Born, E. Wolf, *Principles of Optics* (University Press, Cambridge, 1999)
14. M.A. Ordal, L.L. Long, R.J. Bell, S.E. Bell, R.R. Bell, J.R.W. Alexander, C.A. Ward, Optical properties of the metals Al, Co, Cu, Au, Fe, Pb, Ni, Pd, Pt, Ag, Ti, and W in the infrared and far infrared. *Appl. Opt.* **22**(7), 1099–1119 (1983)
15. M.I. Stockman, Nanofocusing of optical energy in tapered plasmonic waveguides. *Phys. Rev. Lett.* **93**, 137404-1-4 (2004)
16. C. Ropers, C.C. Neacsu, T. Elsaesser, M. Albrecht, M.B. Raschke, C. Lienau, Grating-coupling of surface plasmons onto metallic tips: a nano-confined light source. *Nano Lett.* **7**, 2784–2788 (2007)
17. E. Verhagen, M. Spasenovic, A. Polman, L. Kuipers, Nanowire plasmon excitation by adiabatic mode transformation. *Phys. Rev. Lett.* **102**(20), 203904-4 (2009)
18. L.D. Landau, E.M. Lifshitz, *Electrodynamics of Continuous Media* (Pergamon, Oxford and New York, 1984)